https://doi.org/10.1016/j.apenergy.2017.05.099

Investigation of Demand Response Potentials of Residential Air Conditioners in Smart Grids Using Grey-box Room Thermal Model

Maomao Hu, Fu Xiao*, Lingshi Wang

Department of Building Services Engineering, The Hong Kong Polytechnic University, Kowloon, Hong Kong

Abstract

Over the last few years, the development of information and communication technologies has provided a great opportunity for the residential sector to take part in demand response (DR) programs in smart grids (SGs). Optimal load scheduling via home energy management systems (HEMSs) is a typical technique used to reduce the power consumptions during the DR events. One of the major challenges faced by the HEMS manufacturers and the electric utilities is the lack of an accurate yet convenient tool for predicting the power consumptions of residential homes, particularly the air conditioners, for decision-makings. The aim of this paper is to develop an accurate self-learning grey-box room thermal model and use it to investigate DR potentials of residential air conditioners (ACs). The readily available indoor air and outdoor air temperatures in today's HEMSs are used to train the room thermal model. The model parameters are pre-estimated and scaled to improve the optimization accuracy and computational efficiency. Three optimization techniques including trust region algorithm (TRA), genetic algorithm (GA) and particle swam optimization (PSO) are employed to identify the model parameters separately and their performances are compared. A case study shows that the room thermal model can accurately predict the indoor air temperature profile. Two types of DR strategies of residential ACs, i.e. temperature set-point reset and precooling, are then tested using

* Corresponding author. Tel.: +852 2766 4194; Fax: +852 2765 7198

E-mail address: linda.xiao@polyu.edu.hk

the room thermal model and a simplified air conditioner energy model. Simulation results show that temperature set-point reset combined with precooling strategy can result in more than 26% power reduction during the DR hours on a typical summer day in Hong Kong, without significant change of thermal comfort.

Keywords: Residential air conditioners; Grey-box room thermal model; Demand response; Smart grid; Home energy management system; Particle swarm optimization

Nomenclature

A	area, m^2
AC	air conditioner
c	scaled thermal capacitance, ranging from 0 to 1
C	equivalent overall thermal capacitance, J/K
DR	demand response
EIR	energy input ratio of AC, the inverse of *COP*
ETP	equivalent thermal parameter model
f	radiative/convective split for heat gain
GA	genetic algorithm
HEMS	home energy management system
I	global solar radiation, W/m^2
OM	order of magnitude of parameter value
PSO	particle swarm optimization

Q	heat gain, W
r	scaled thermal resistance, ranging from 0 to 1
R	equivalent overall thermal resistance, K/W
S	AC on-off signal
SG	smart grid
$SHGC$	Solar Heat Gain Coefficient
T	temperature, ℃
TRA	trust region algorithm
U	heat transfer coefficient, W/(m^2·K)
WWR	window-to-wall area ratio

Greek symbols

α	absorptance of surface for solar radiation
ζ	searching factor, ranging from 0 to 1
δ	dead band for AC control
σ	thickness, m
ρ	density, kg/m^3

Subscripts

cap	cooling capacity of AC
db	air dry bulb temperature

est	estimated values
ex	external
i	indoor air
in	wall internal surface
inter	internal
lb	lower bounds
m	internal thermal mass
nom	nominal operation condition
o	outdoor air
set	set-point
ub	upper bounds
w	wall
wb	air wet bulb temperature
win	window

1. Introduction

Smart grid is an intelligent electric system that integrates with advanced communication and control technologies, transforming the current grid to one that is cleaner and more efficient, reliable, resilient and responsive [1, 2]. Demand response (DR), facilitated by smart grids, can achieve reductions in the peak loads, energy consumptions, and carbon emission [3-5]. Besides, it can facilitate greater penetrations of intermittently available renewable resources (solar and wind in particular) [6, 7].

According to the U.S. Energy Information Administration, demand response programs provided 13,036MW actual peak reductions in 2015 in total, and the residential sector provided 26% of the total peak reductions [8]. As indicated by Federal Energy Regulation Committee, it is the residential class that represents most untapped potentials for demand response, and the residential customers are able to provide over 45 percent of the potential impacts in 2019 [9]. Residential DR plays an important role in the potential DR resources [10-13]. Residential air conditioners (ACs), as the major contributors to the home electricity bills, have been attracting increasing interest in exploiting the DR potentials of residential homes.

Both electric utilities and smart home energy management systems (HEMSs) requires the predictions of power reductions of residential ACs to implement DR strategies. For the former, many influential decisions on grid operations are made based on the predicted power reduction, such as generation and reserve planning, dynamic electricity prices and payments to homes joining DR program [14,15]. Taniguchi et al. evaluated the effects of electricity saving measures on peak demand reductions in the Japanese residential sector on a region scale (5000 households) based on a bottom-up type model [16]. Widergren et al. discussed the design of the electricity rate, and simulated the DR resources at the distribution level where the residential consumers and household appliances can receive real-time pricing signals [17]. For the latter, the widely adopted optimal load scheduling methods for DR in the presence of dynamic electricity pricings are also developed based on the predication of AC power consumption. To determine the optimal balance between hourly electricity prices and the use of smart household appliances, Lujano-Rojas et al. proposed an optimal load management strategy which considered predictions of electricity prices, energy demand and renewable power productions [18]. Molina et al. developed an optimization methodology, which includes system identification, model-

predictive control and genetic algorithm, to achieve an acceptable compromise between comfort and cost in the presence of dynamic electricity prices [19]. Room thermal models are necessary to predict the power consumption and power reduction of residential ACs.

Different types of room thermal models have been applied for residential DR purpose. Building simulation softwares, such as EnergyPlus in [20], and eQUEST in [21], were used to simulate the room thermal dynamics under different DR control strategies. A large amount of building parameters are required as inputs in the simulation softwares, which is difficult even for the newly designed buildings. Besides, it is extremely time-consuming when investigating the DR resources of a population of homes on a region scale. Another room thermal model is the widely-used equivalent thermal parameter (ETP) model, which simplifies the room thermal dynamics as a second-order electric circuit analog. Lu and Katipamula [22, 23] used the ETP model to study the impacts of various residential air conditioner control strategies on electric distribution feeder load profile during the DR periods for a single residence and a number of residences separately. Based on the ETP model, Thomas et al. [24] proposed an intelligent residential AC system controller to provide optimal comfort and cost trade-offs for the residents. The ETP model was also adopted by Zhang et al.[25] to describe the thermal dynamics of each individual load and deal with a number of heterogeneous loads. Besides, GridLAB-D, an open-source power systems modeling and simulation environment, also uses the ETP model to simulate the AC energy consumptions during the DR events [26]. However, there are two main critical issues about the ETP model. First, the model is too simplified to consider the impacts of specific building features such as wall material, window arrangement, and internal thermal mass. Second, the values of the ETP model parameters were determined according to the room geometry and thermal parameters in a database developed over 20 years ago [27]. The room thermal parameters

are only applicable to the residential buildings in the US. The architecture design and envelop thermal properties are very different from the high-rise residential buildings in modern cities like Hong Kong and Shanghai. The uncertainties of the parameters have significant impacts on the accuracy of the modelling results.

The present study aims to develop an accurate self-learning grey-box room thermal model and the associated parameter identification methods for investigating DR resources from residential air conditioners (ACs). Three major contributions are made in this study. First, we developed an accurate grey-box room thermal model for predicting the indoor air temperature under dynamic operating conditions. The model parameters can be learnt by making effective use of the data available in the today's smart in-home sensors. Second, we proposed pre-estimation and scaling approaches to pre-processing the model parameters, which help to improve the accuracy and computational efficiency of the parameter identification process. We also compared three popular optimization techniques including trust region algorithm (TRA), genetic algorithm (GA) and particle swam optimization (PSO) for parameter identification. Third, the room thermal model was integrated with a simplified air conditioner energy consumption model to test two types of DR strategies of residential ACs, i.e. temperature set-point reset and precooling. Due to the simple structure and moderate computation load, the developed room thermal model is suitable for the applications in the HEMSs, such as model-based AC load scheduling in response to DR signals. This work is also valuable for electric utilities to evaluate the impacts of DR programs on large populations of residential ACs and make appropriate incentive policies.

The structure of this paper is organized as follows. In Section 2, an improved grey-box model is developed, identified and validated. Three optimization techniques are adopted separately to identify

the model parameters and their performances are compared. A flowchart of the parameter identification process is provided. In Section 3, the room thermal model is integrated with a AC model for investigating the popular DR strategies of residential air conditioners. Six cases are created for the following simulation study, including one baseline case (i.e. without demand response strategy) and the five DR cases adopting the strategies of temperature set-point reset and precooling, respectively. Section 4 presents the simulation results in the six cases in terms of indoor temperature profile, power reduction and electricity consumption on a typical hot summer day. A simplified AC energy consumption model is adopted in the simulation study. Finally, the conclusions and the future work are presented in Section 5.

2. Grey-box room thermal model

In this section, a grey-box room thermal model is developed, identified and validated. The developed model contains more physical principles of the room thermal dynamics. Besides, it can make full use of the indoor air temperature data from smart in-home sensors to identify the unknown model parameters with the support of data-driven optimization techniques.

2.1. Model development

The physical description of a grey-box model should be neither too simple nor too complex. It should capture adequate room thermal behaviors to keep its robustness to different operation conditions. It also should not be too complicated for saving computation time. In general, the room thermal dynamics can be expressed as a set of first-order ordinary differential equations containing several uncertain parameters to be identified. It is worth to mention that the physical meanings of the parameters in different grey-box models are different, depending on how the target zone is divided.

Fig.1 illustrates the components included in the model and the heat fluxes exchanged between them. The model mainly contains four parts, i.e. outdoor environment, building envelope, indoor air, and internal thermal mass.

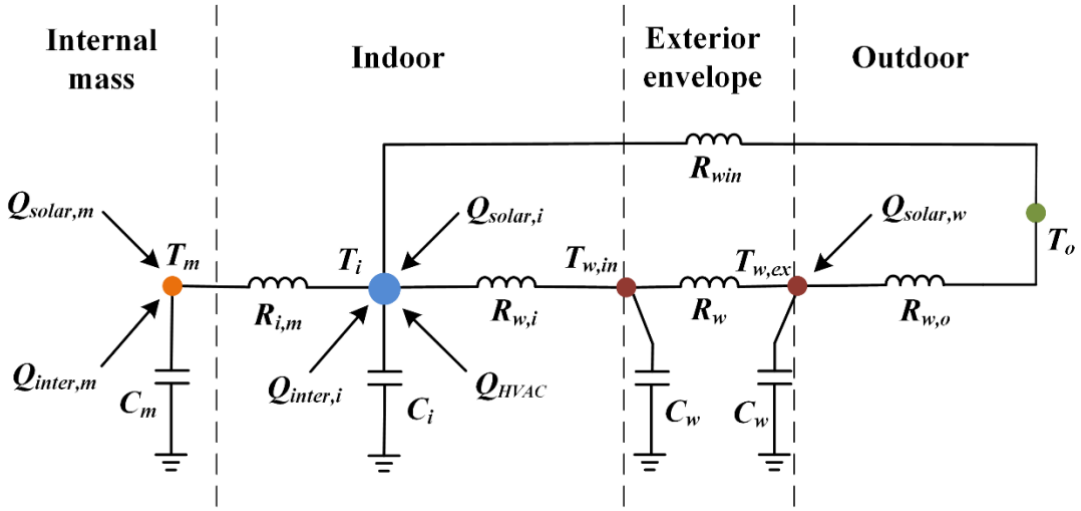

Fig. 1. Schematic of the grey-box thermal model of residential buildings (5R4C).

The exterior building envelop consists of opaque walls and transparent windows. Considering the climate in Hong Kong, most residential buildings are constructed with light-weight wall and without thermal insulation. Therefore, it is reasonable to consider the external wall as one thermal resistance and two equal thermal capacitances [28]. Two types of heat transfer on the external wall surface are considered, i.e. convective heat transfer with the outdoor air and radiative heat transfer with the sky. Heat flows through the windows consist of 1) conductive and convective heat transfer caused by the temperature difference between outdoor and indoor air, 2) solar radiation incident on the windows, either directly from the sun or reflected from the ground or adjacent buildings. Then a portion of solar radiation through the window is directly transmitted into indoor air, and the rest is absorbed by internal thermal mass constituted by floor, ceiling, partitions and furniture. The bulk of internal mass absorbs the solar radiation through the windows and the heat from indoor heat sources, then gradually transfers the heat into the space by convection. The air in the interior zone, which exchanges heats

with the internal thermal mass, internal wall surface and outdoor air through windows, is represented by a lumped node. Besides, the energy from the solar radiation, HVAC system, and internal heat sources (e.g. occupants, lights, and equipment) is assumed to be immediately absorbed by the indoor air.

The energy balances for the external/internal wall surfaces, the indoor air and the internal thermal mass are given by the following equations:

$$C_w \frac{dT_{w,ex}}{dt} = \frac{T_o - T_{w,ex}}{R_{w,o}} + \frac{T_{w,in} - T_{w,ex}}{R_w} + Q_{solar,w} \quad (1)$$

$$C_w \frac{dT_{w,in}}{dt} = \frac{T_{w,ex} - T_{w,in}}{R_w} + \frac{T_i - T_{w,in}}{R_{w,i}} \quad (2)$$

$$C_i \frac{dT_i}{dt} = \frac{T_m - T_i}{R_{i,m}} + \frac{T_{w,in} - T_i}{R_{w,i}} + \frac{T_o - T_i}{R_{win}} + Q_{solar,i} + Q_{inter,i} + Q_{HVAC} \quad (3)$$

$$C_m \frac{dT_m}{dt} = \frac{T_i - T_m}{R_{i,m}} + Q_{solar,m} + Q_{inter,m} \quad (4)$$

$$Q_{solar,w} = \alpha A_w I_{solar} \quad (5)$$

$$Q_{solar,m} = f_{solar,m} \times SHGC \times A_{win} I_{solar} \quad (6)$$

$$Q_{solar,i} = f_{solar,i} \times SHGC \times A_{win} I_{solar} \quad (7)$$

$$Q_{inter,i} = f_{inter,i} Q_{inter} \quad (8)$$

$$Q_{inter,m} = f_{inter,m} Q_{inter} \quad (9)$$

where R and C represent the thermal resistance and thermal capacitance, respectively; T denotes temperature; subscripts *i, o, w, in, ex, win* and *m* indicate indoor air, outdoor air, exterior wall, internal wall surface, external wall surface, window and internal mass, respectively; $Q_{solar,w}$, $Q_{solar,i}$ and $Q_{solar,m}$ are solar heat gains absorbed by external wall surface, indoor air and internal mass, respectively; $Q_{inter,i}$ and $Q_{inter,m}$ are internal heat gains absorbed by indoor air and internal mass, respectively; I_{solar} denotes global solar radiation; A denotes geometric area; f denotes the radiative/convective split for

heat gain; α denotes absorptance of surface for solar radiation; *SHGC* denotes solar heat gain coefficient. To improve the accuracy of the model, the equations in the model include more physical parameters compared with other RC models, such as *SHGC*, α, and *f*. The values of *SHGC* and α are determined by the materials, structures and processes of the glasses and external wall surface [29]. The radiative/convective splits for different types of heat gains are different [29].

In the grey-box model, *R* and *C* are free parameters which need to be identified based on historical data. There are two points that should be noticed. 1) The free parameters for a time-invariant model are not functions of time, although the values of the parameters actually change with time or under different weather conditions. For instance, when the outdoor wind speed increases, the convective heat transfer coefficient between the external wall surface and the outdoor air increases as well. The changes of these free parameters are so small that they are assumed to be fixed instead of being function of time. 2) *R* and *C* characterize the building inherent thermal features. It will make no difference to the identification results whether or not the heat gains from internal sources or HVAC are considered.

2.2. Parameter identification

In order to improve the accuracy and computation efficiency of the optimizations, the parameter pre-processing and different optimization techniques are proposed in this study. The optimal parameters can be accurately and efficiently obtained by the systematic identification procedure which is shown in Figure 2.

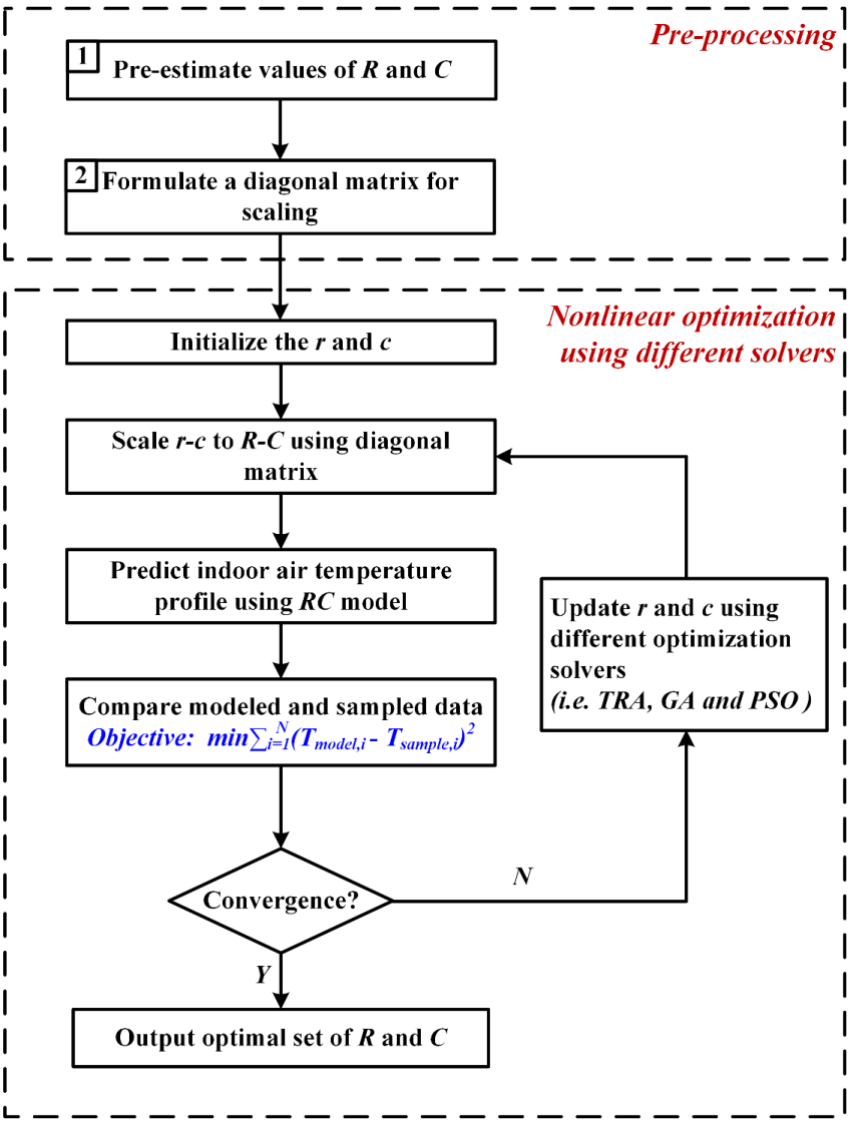

Fig. 2. Flowchart of parameter identification for the grey-box model.

2.2.1. Parameter pre-processing

The model robustness relies on not only the feasible physical structure but also the reasonable values of R and C. To make the trained R and C values reasonable and acceptable, they are estimated based on the surveyed values of the thermal parameters of residential buildings in Hong Kong and the specific geometric size of the room. With the pre-estimated values, the search ranges for the parameters can be narrowed down and thus the computation time for optimization also can be saved.

In Hong Kong, U-value of the exterior wall typically ranges from 2.2 to 2.9 W/(m^2·K), and average U-value of the single glazed window is 5.6 W/(m^2·K). Considering the average wind speed of 7.2 m/s

during summer in Hong Kong, an average heat transfer resistance of the external wall surface is recommended as 0.036 (m^2·K)/W [30, 31]. Typical range for the heat transfer resistance of the interior surface is from 0.12 to 0.2 (m^2·K)/W [29]. Thermal resistances, i.e. R_w, R_{win}, $R_{w,o}$, $R_{w,i}$, and $R_{i,m}$, are all overall thermal resistances, and can be calculated by Eq. (10). Equivalent thermal capacitances including C_i, C_w, and C_m play functions of dampening the effects of heat transfer. Without them, instantaneous temperature changes in corresponding objects would occur. The building internal mass (e.g. partitions, furniture, carpet, etc.) can be summed to a lumped thermal mass C_m, ranging from 100 to 450 kJ/(K·m^2) [32, 33]. Thermal capacitance of half exterior wall can be calculated by Eq. (11). With the estimated values of R and C, the search range of parameter then can be determined by adopting a search factor ζ ranging from 0 to 1. The upper and lower bounds of the search range can be calculated by Eqs. (12) - (13).

$$\mathrm{R} = \frac{1}{\mathrm{A} \times \mathrm{U}} \tag{10}$$

$$C_w = \frac{\sigma_w A_w \rho_w c_w}{2} \tag{11}$$

$$R_{ub} = (1 + \zeta) \times R_{est} \tag{12}$$

$$R_{lb} = (1 - \zeta) \times R_{est} \tag{13}$$

After pre-estimating the parameter values, we can easily find the orders of magnitudes (OM) of R and C vary a lot, namely the parametric model is poorly scaled. Poorly scaled problems usually arise in the simulation of physical and chemical systems where different processes take place at different rates [34]. In the simulation of building thermal dynamics, the cost function is not the same sensitive to the changes of R and C. To solve this problem, a scaling method, i.e. diagonal scaling, is introduced to make the solution more balanced. As shown in Eq. (14), the diagonal matrix can transform the

poorly scaled variables to new variables within an order of magnitude of 1. The diagonal elements are orders of magnitudes of the estimated *R* and *C*.

$$\begin{pmatrix} C_w \\ C_i \\ C_m \\ R_{win} \\ R_w \\ R_{w,o} \\ R_{w,i} \\ R_{i,m} \end{pmatrix} = \begin{pmatrix} OM_1 & \cdots & 0 \\ \vdots & \ddots & \vdots \\ 0 & \cdots & OM_8 \end{pmatrix}_{8\times 8} \begin{pmatrix} c_w \\ c_i \\ c_m \\ r_{win} \\ r_w \\ r_{w,o} \\ r_{w,i} \\ r_{i,m} \end{pmatrix} \tag{14}$$

2.2.2. Optimization techniques for model identification

Searching optimal values of the undetermined parameters in a grey-box model is a nonlinear optimization process. Given a set of *R* and *C*, the grey-box model can predict the indoor air temperature profile. An objective function can be used to evaluate the fitness between the predicted data and the measured data collected from smart in-home sensors during the optimization process. The optimization objective is to minimize the integrated root-mean-square error, as defined in Eq. (15).

$$J(C_w, C_i, C_m, R_{win}, R_w, R_{w,o}, R_{w,i}, R_{i,m}) = minimize\sqrt{\frac{1}{N}\sum_{i=1}^{N}(T_{model,i} - T_{sample,i})^2} \tag{15}$$

where $T_{model,i}$ is the predicted indoor air temperature, $T_{sample,i}$ is the actual measured indoor air temperature and the C_w, C_i, C_m, R_w, R_{win}, $R_{w,o}$, $R_{w,i}$, $R_{i,m}$ are the unknown parameters of the grey-box model.

Optimization techniques are required to find the optimal values of R and C which make the objective function reach the minimal value. Three types of optimization solvers including a mathematical solver i.e. trust region algorithm (TRA) , and two evolutionary solvers, i.e. genetic algorithm (GA) and particle swarm optimization (PSO) , are employed to identify the RC values in this study. Both GA

[19, 35-37] and PSO [38] have been used to solve the optimization problems in the domain of HVAC. In this study, all optimizations are carried out in MATLAB, and performed on a desktop computer with Intel Core i7-4790 (3.60 GHz), 16 GB of memory, under Windows 10 64-bit operating system. Runtimes and optimization results of these three optimization strategies will be compared in the real cases in subsection 2.3.

2.3. Model validation

One residential bedroom in Hong Kong was chosen to test the grey-box room thermal model. The geometric dimension of the room is 4.8m long, 3.6m wide, and 3m high. It has only one exterior wall in which single glazed windows are embedded. The Window-Wall-Ratio (*WWR*) is 0.2 and the type of glass is clear. The absorption coefficient of the external wall surface is 0.8, and the solar heat gain coefficient (*SHGC*) of the glass is 0.7. Considering the interior shading and the types of internal heat gains, the radiative/convective splits for both solar heat gains through the windows and internal heat gains are 0.5/0.5 [29]. A smart sensor was installed in the room to record the indoor air temperature with the interval of 10 minutes. For the outdoor weather data, both outdoor air temperature and horizontal global solar radiation are obtained from the nearby Hong Kong Observatory with the interval of 1 minute.

Parameter pre-estimations are first conducted using the specific geometric parameters and general building thermal parameters in Hong Kong, as listed in Table 1. The search range of each parameter is set as 1±30% of the corresponding estimated value. To improve the search efficiency, the estimated *R* and *C* are transformed to r and c, ranging from 0 to 1, by a diagonal matrix, as shown in Eq. (16).

Table 1

Pre-estimations of R and C based on prior knowledge.

	C_w (J/K)	C_i (J/K)	C_m (J/K)	R_{win} (K/W)	R_w (K/W)	$R_{w,o}$ (K/W)	$R_{w,i}$ (K/W)	$R_{i,m}$ (K/W)
Estimated values	1,850,688	187,868	25,488,000	0.0643	0.0463	0.0033	0.0106	0.0014
Orders of magnitudes	1E+07	1E+06	1E+08	1E-01	1E-01	1E-02	1E-01	1E-02

$$OM = \begin{pmatrix} 10^{7} & & & & & & & \\ & 10^{6} & & & & & & \\ & & 10^{8} & & & & & \\ & & & 10^{-1} & & & & \\ & & & & 10^{-1} & & & \\ & & & & & 10^{-2} & & \\ & & & & & & 10^{-1} & \\ & & & & & & & 10^{-2} \end{pmatrix}_{8\times 8} \quad (16)$$

Three optimization solvers, i.e. TRA, GA and PSO, are used to identify the parameters. A five-day (27 - 31 July 2015) indoor air temperature profile is used for the identification. Noted that the time step of the prediction is 1minute and the predicted profile is reinitialized to the sampled value in the midnight of each day to reduce the accumulative error. The identification results and runtimes of the three optimization methods are listed in Table 2. Then, another five-day (1 - 5 August 2015) indoor air temperature profile is forwardly predicted using the developed grey-box model and the identified *R* and *C*.

Table 2

Identification results using different optimization solvers.

Optimization solver	Runtime (minute)	Identification results							
		C_w (J/K)	C_i (J/K)	C_m (J/K)	R_{win} (K/W)	R_w (K/W)	R_{wo} (K/W)	R_{wi} (K/W)	R_{im} (K/W)
TRA	7.8	2,221,000	225,400	30,590,000	0.04500	0.05312	0.00233	0.00745	0.00095
GA	87.7	2,189,700	223,710	30,391,000	0.04580	0.04830	0.00230	0.00870	0.00091
PSO	24.3	2,220,800	225,440	30,585,600	0.04500	0.04780	0.00230	0.00740	0.00090

In order to quantify the deviations of the predicted data from the measured data during both training session and validation session, three indices are used to evaluate the deviations, as defined in Eqs. (17) - (19). Table 3 lists the indoor air temperature deviations of the modeled data from the measured data using different optimization solvers.

Mean Absolute Error

$$MAE = \frac{1}{n}\sum_{i=1}^{n}\left|T_{model,i} - T_{sample,i}\right| \tag{17}$$

Mean Absolute Percentage Error

$$MAPE = \frac{1}{n}\sum_{i=1}^{n}\left|\frac{T_{model,i}-T_{sample,i}}{T_{sample,i}}\right| \tag{18}$$

Root Mean Square Error

$$RMSE = \sqrt{\frac{1}{n}\sum_{i=1}^{n}(T_{model,i} - T_{sample,i})^2} \tag{19}$$

Table 3

Deviations of the modeled data from the measured data using different optimization solvers.

Optimization solver	Training session			Validation session		
	MAE	MAPE	RMSE	MAE	MAPE	RMSE
TRA	0.1968	0.63%	0.2475	0.2276	0.72%	0.2849
GA	0.1981	0.63%	0.249	0.2293	0.72%	0.2867
PSO	0.1952	0.62%	0.2459	0.2243	0.71%	0.2813

Comparing the optimization results in Table 3, it can be seen that the optimal parameter values by different optimization methods are almost the same. The least runtime is around 7.8 minutes, achieved by the mathematical optimization solver, TRA, and the GA solver takes the longest runtime. The least deviations between the modeled data and measured data are achieved by the optimization strategy of PSO, as shown in Table 4. The outdoor weather conditions during the training and validation sessions

are shown in Fig. 3-a and Fig. 4-a, respectively. The sampled indoor air temperature profiles and the modeled profiles using the PSO optimization results for training and validation sessions are shown in Fig. 3-b and Fig. 4-b, respectively.

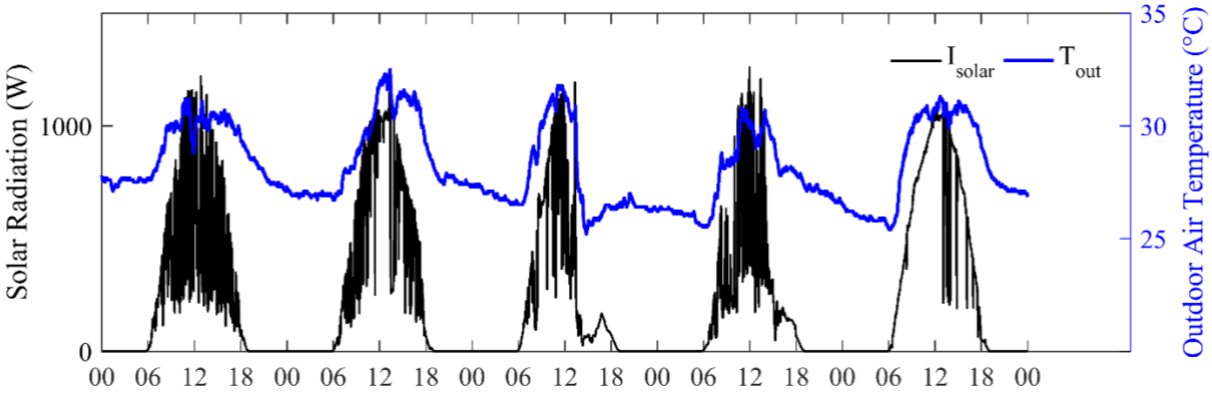

Fig. 3-a. Outdoor weather conditions during the training session.

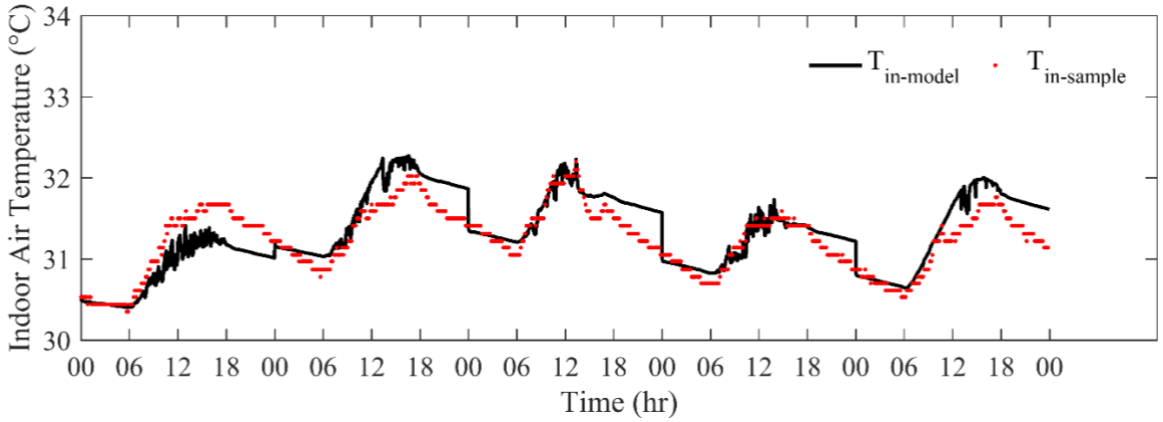

Fig. 3-b. Predicted and sampled indoor air temperature profiles during the training session.

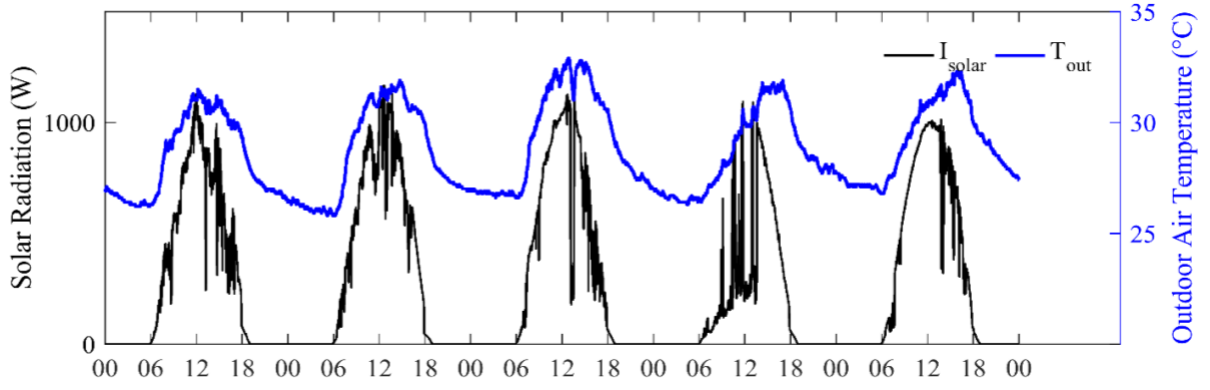

Fig. 4-a. Outdoor weather conditions during the validation session.

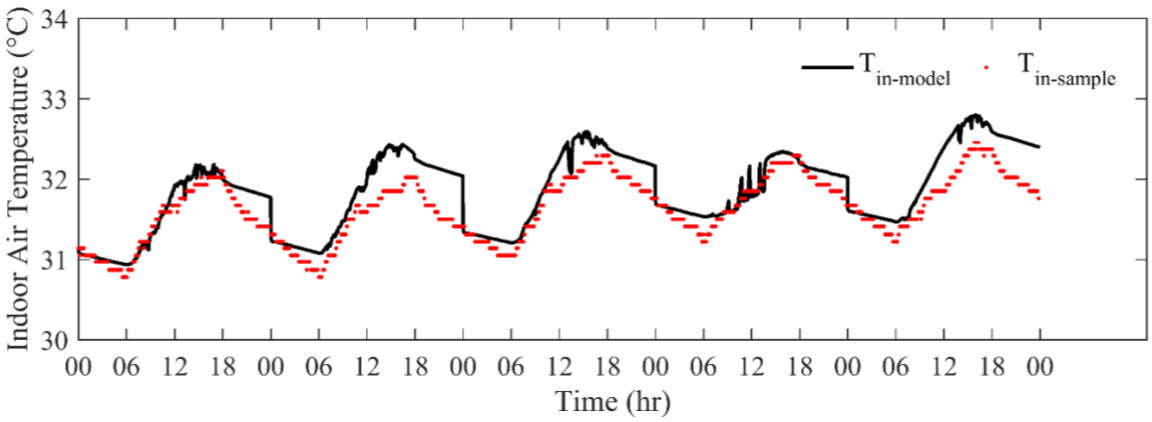

Fig. 4-b. Predicted and sampled indoor air temperature profiles during the validation session.

To better understand the function played by each component in the grey-box model physically, the room thermal dynamics on a typical summer day (1 August 2015) are simulated and shown in Fig. 5. The temperature of the external wall surface ($T_{w\text{-}ex}$) in the daytime is higher than the outdoor air temperature (T_{out}) due to the effects of solar radiation, while at night without the solar radiation it is closer to the outdoor air temperature. The temperatures of the internal thermal mass (T_{mass}) and internal wall surface ($T_{w\text{-}in}$) hardly change simultaneously with the outdoor weather conditions due to the thermal capacitances. It is why the cooling output and hence the power consumption of air conditioners can be reduced during the DR period without significantly affecting the thermal comfort of residents. Fig. 5 shows that the model outputs ($T_{in\text{-}model}$) and the sampled indoor air temperature ($T_{in\text{-}sample}$) agree very well, which means the model can predict the indoor air temperature in a high degree of accuracy.

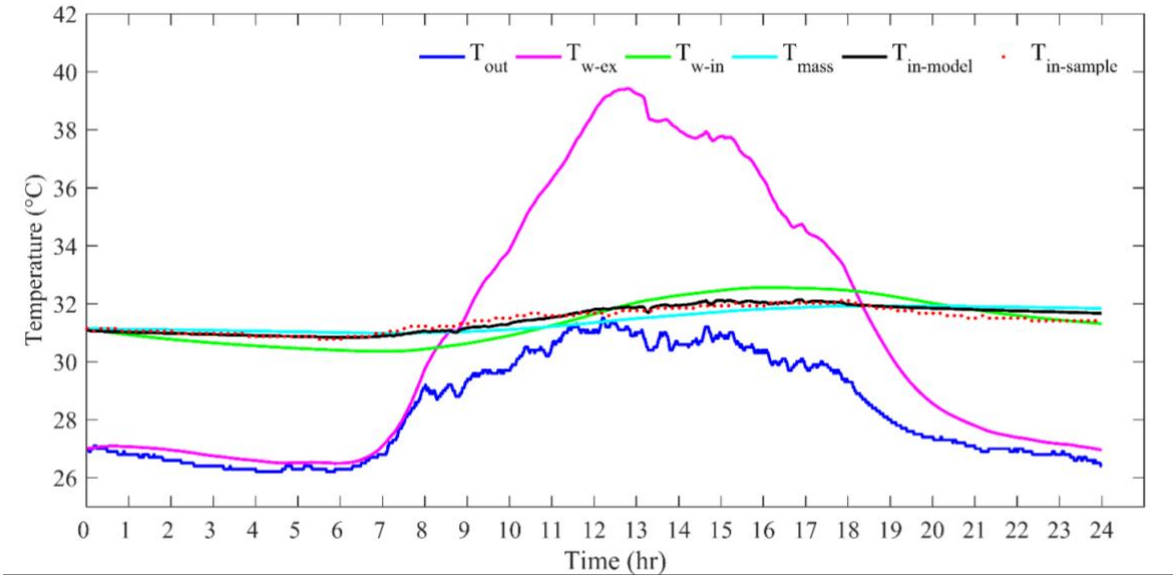

Fig. 5. Comparison of modeled and sampled indoor air temperatures on a typical summer day.

3. DR strategies of residential ACs

Demand response of an electric product is defined as an automatic alteration of normal operation mode in response to an initiating signal from the grid. For residential ACs, the most popular DR strategy is the temperature set-point reset strategy [39, 40]. The indoor air temperature set-point in the AC thermostats or remote controllers is set higher during the DR periods to reduce the AC power consumption, without significantly influencing the thermal comfort of residents due to the thermal mass of rooms. Besides, the AC temperature set-point is set lower in advance to pre-cool the room so that the power consumption can be reduced by adopting a higher set-point during the DR periods.

The control scheme as illustrated in Fig. 6 is proposed for the residential DR-enabled AC towards smart grid. During the DR events, the HEMS receives the DR signals from the electric utilities via smart meters, optimizes the set-point schedules online, and delivers the schedules to the controller of AC. In this paper, we aim to evaluate the DR strategies using the developed model. The development of online optimization of temperature set-point schedule is the focus of our future work. The training data for optimizing the model parameters, including the outdoor air temperature and solar radiation

as well as indoor air temperature, are assumed available in the HEMS. It is a reasonable assumption in the context of modern IT technology. Real-time outdoor weather data are usually available for the public on the local observatory website. The HEMS can collect the weather data via network. The smart in-home wireless sensors can measure the indoor temperature and send it to the HEMS. The parameter optimization process presented above shows that one-week data at the interval of 10 minutes are sufficient for producing an accurate room thermal model.

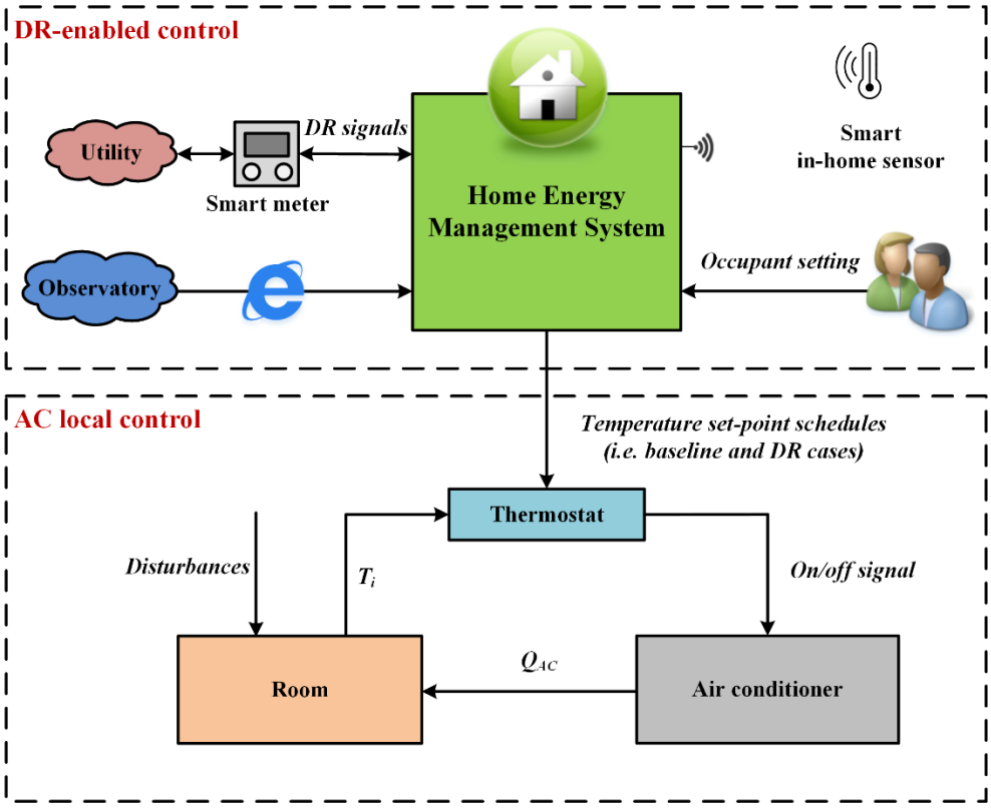

Fig. 6. Control scheme for the residential DR-enabled AC towards smart grid.

The AC control algorithm is the basic on/off control. For this type of AC, the energy consumption during a period of time is mainly determined by the accumulated on-state time. Its state depends on the thermostat set-point and dead-band (δ = 1°C), as shown in Eqs. (20) - (21). It should be noted that in order to protect the compressor, one state must last for at least 3 minutes before it is switched to another state.

$$S = 1,\ T_i > T_{set} + \delta/2 \tag{20}$$

$$S = 0,\ T_i \leq T_{set} - \delta/2 \tag{21}$$

Table 4 lists six predefined control strategies of ACs, i.e. one baseline case and five DR cases. The baseline case employs a constant temperature set-point of 24℃ as long as the room is occupied. In the DR Case 1 and Case 2, the temperature set-points are reset from 24℃ to 25℃ and 26℃ respectively during the DR periods. In the DR Case 3, Case 4 and Case 5, the room is also precooled for one hour except that the temperature set-points are reset during the DR hours.

Table 4

Indoor air temperature set-point schedules for different DR strategies.

Operation Cases	Temperature set-point schedules		
	Normal period	Precooling Period	DR Period
Baseline Case	24	off	24
DR Case 1 *(Reset)*	24	off	25
DR Case 2 *(Reset)*	24	off	26
DR Case 3 *(Precooling + reset)*	24	25	25
DR Case 4 *(Precooling + reset)*	24	26	26
DR Case 5 *(Precooling + reset)*	24	26	25

4. Simulation studies

Apart from the room thermal model, a power consumption model of residential ACs is also required for energy analysis. In general, the existing methods for modeling AC energy consumption can be divided into two categories: empirical modeling and numerical modeling. In this study, one empirical correlation provided by DOE-2, a widely used and accepted building energy analysis program [41], is chosen to predict the AC performances under different operation conditions. Dimensionless factors

for cooling capacity and *EIR* are functions of the wet-bulb temperature of the indoor air ($T_{in,wb}$) and the dry-bulb temperature of the outdoor air ($T_{o,db}$). The recommended values of the dimensionless factors can be found from DOE-2 [41]. Considering the varies of the temperature and the humidity of the indoor air are relatively small, the $T_{in,wb}$ is assumed to be at the standard test condition 19.4 ℃. Noted that the standard test conditions are: $T_{i,db}$ = 26.7 ℃, $T_{i,wb}$ = 19.4 ℃, $T_{o,db}$ = 35 ℃ , $T_{o,wb}$ = 23.9 ℃ [42]. Therefore, the real cooling capacity (*cap*) and *EIR* in the given operation condition can be expressed by Eqs. (22) – (23).

$$cap = (-0.0092T_{o,db} + 1.3243)cap_{nom} \tag{22}$$

$$EIR = (0.0193T_{o,db} + 0.3259)EIR_{nom} \tag{23}$$

One residential air conditioner with a nominal cooling capacity of 2.8 kW and a nominal *COP* of 2.5 is chosen, and its DR potential is investigated on a typical hot summer day (i.e. 1 August 2015). The outdoor weather conditions and internal heat gains are shown in Fig. 7-a. There are no internal heat gains from 8:00 to 18:00, as the occupants are out for school or work during that time. Demand response signals, which normally last for 2 to 4 hours, are determined and delivered by the electric utilities. In the present paper, the DR event is assumed to be from 18:00 to 20:00, which are the typical DR hours in Hong Kong. The precooling approach in the present paper is to turn on the AC before the occupants come back home (e.g. 17:00 – 18:00).Noted that the simulation starts from midnight, as the room thermal dynamics have been stable for a long time. The initial value of indoor air temperature can then be set as the AC temperature set-point. Besides, the time step for simulation is set as 1 minute.

4.1. Baseline case

The baseline of AC power consumption under the conventional operation pattern, i.e. without DR, is first simulated. In the baseline case, AC keeps working to maintain the indoor air temperature around the set-point 24 ℃ when the room is occupied from 18:00 to 8:00 of next day. It is worth to mention that the average electric power consumption (kW) during a period of half an hour is used for analysis, which equals the accumulated power consumption divided by corresponding time duration. Fig. 7-b shows the AC on/off state and the electricity consumption profiles in the conventional operation pattern. As can be seen from the figure, a power spike occurs at the beginning of DR hours. The electricity consumption during the DR hours is obviously higher that the consumption during the non-DR hours due to the operation of AC. The aim of the DR strategies is to reduce the AC power consumptions during the DR hours.

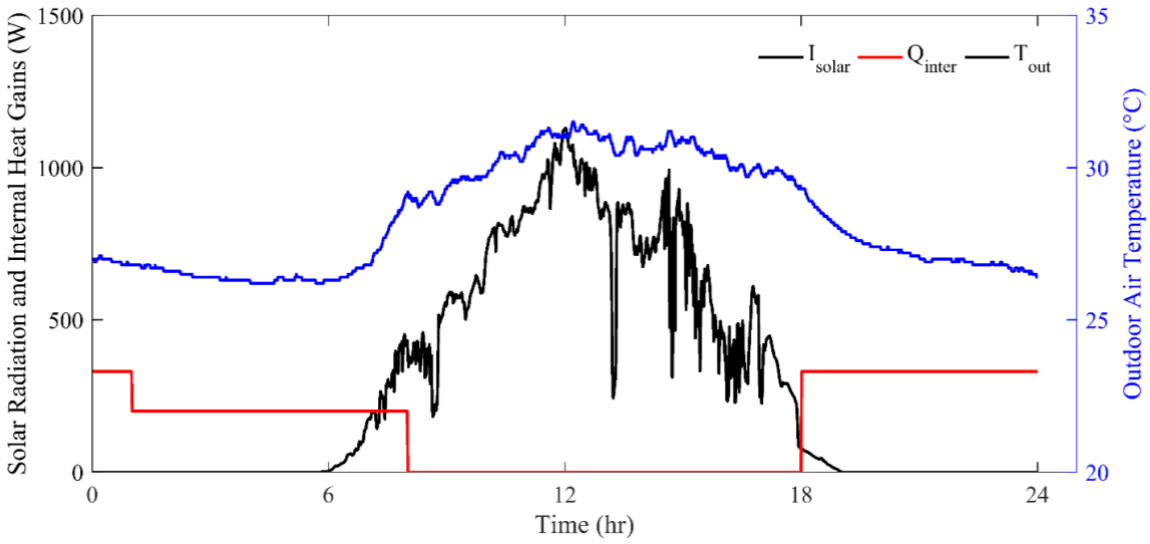

Fig. 7-a. Outdoor weather conditions and internal heat gains on a typical hot summer day

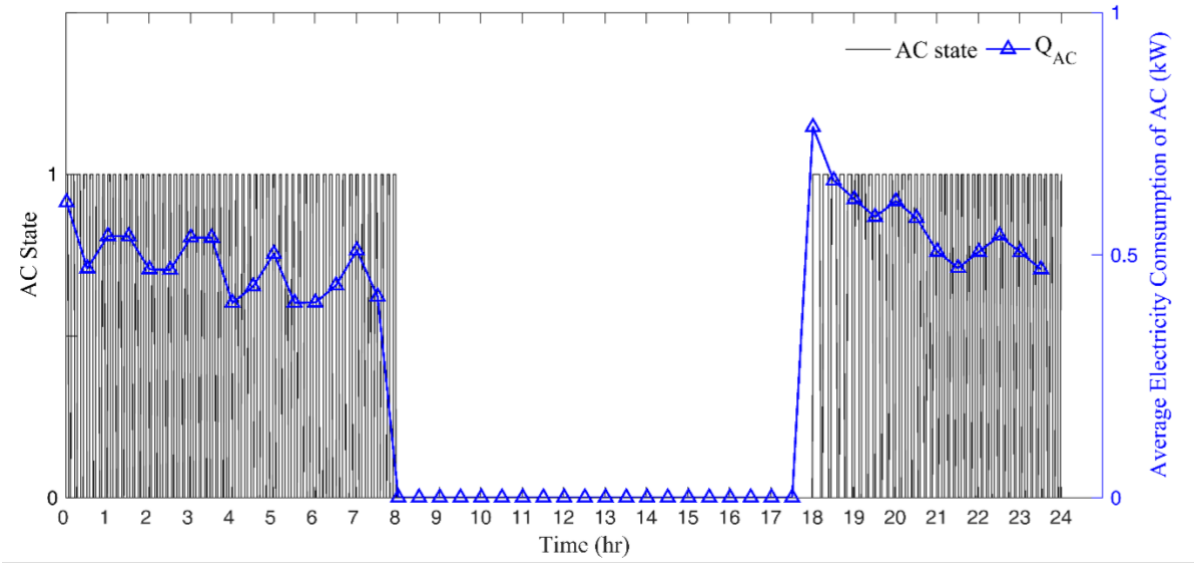

Fig. 7-b. AC on/off state and power consumption profiles in the baseline case

4.2. DR cases

As listed in Table 4, based on the popular DR control strategies, i.e. temperature set-point reset and precooling, five DR cases are proposed to reduce the peak power and power consumption during the DR hours. They are evaluated using the developed room thermal model. Fig. 8 shows the indoor air temperature profiles in the baseline case and DR cases. The indoor air temperatures in all cases are able to reach the temperature set-points and fluctuate around the setpoints. In the first three cases, the indoor air starts to be cooled from 18:00. In contrast, in the last three cases the indoor air is precooled since from the 17:00, providing the potentials in power reductions during the DR periods.

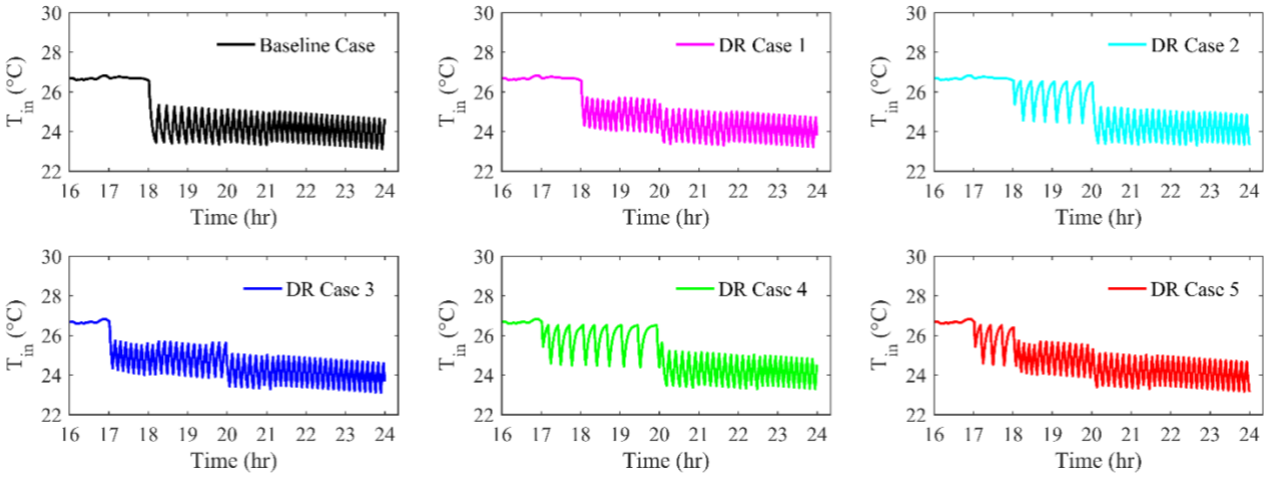

Fig. 8. Indoor air temperature profiles in the baseline and DR cases

In terms of the energy consumption, as can be seen from Fig. 9 and Table 5, when the thermostat set-points are reset from 24℃ to 25℃ and 26℃ during the DR periods, power reduction percentages of 24.62% and 66.15% can be achieved by DR Case 1 and DR Case 2, respectively. Therefore, residential AC power during the DR hours can be reduced via the temperature set-point reset control strategies.

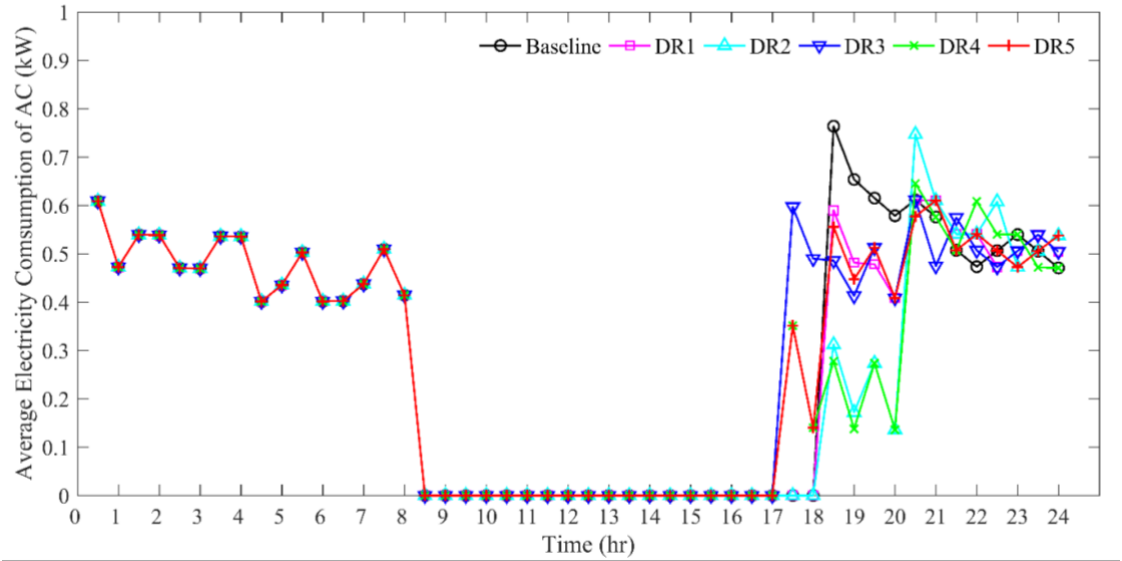

Fig. 9. AC power consumption profiles in the baseline and DR cases

In addition, the precooling strategy can help to further reduce the power consumption during the DR hours. In contrast to DR case 1 and 2, peak reductions during the DR hours in DR Cases 3, 4, and 5

have certain increases. Compared with the DR Case 1 which has the same set-point with DR case 3, the peak demand reduction percentage in DR Case 3 rises from 24.62% to 30.77%. Similarly, the precooling procedure enables the power reduction percentage increases from 66.15% in DR case 2 to 67.69% in DR Case 4. Comparing the DR Case 3 and DR Case 5, it can be found that the set-point during the precooling period has impact on the demand reduction during DR periods. When the set-point during the precooling session increases from 25℃ to 26℃, the AC contribution to the peak demand reduction will decrease from 30.77% to 26.15%. In conclusion, the precooling control strategy can help to further reduce the power consumption during the DR hours. Although the precooling strategy consumes more energy during the precooling period compared with the baseline case, the all-day energy consumptions may not be necessarily larger than the baseline energy consumption, due to a higher temperature set point during the DR period.

Table 5

AC energy consumption pattern in the baseline and DR cases.

Cases	Energy consumption (kWh)			Average power consumption during DR periods (kW)	Power reduction percentage during DR periods
	Precooling period (17:00–18:00)	DR period (18:00-20:00)	All-day		
Baseline case	0	1.31	7.24	0.65	0.00%
DR Case 1 *(Reset)*	0	0.98	6.98	0.49	24.62%
DR Case 2 *(Reset)*	0	0.45	6.56	0.22	66.15%
DR Case 3 *(Precooling + reset)*	0.54	0.91	7.38	0.45	30.77%
DR Case 4 *(Precooling + reset)*	0.25	0.41	6.67	0.21	67.69%
DR Case 5 *(Precooling + reset)*	0.25	0.96	7.17	0.48	26.15%

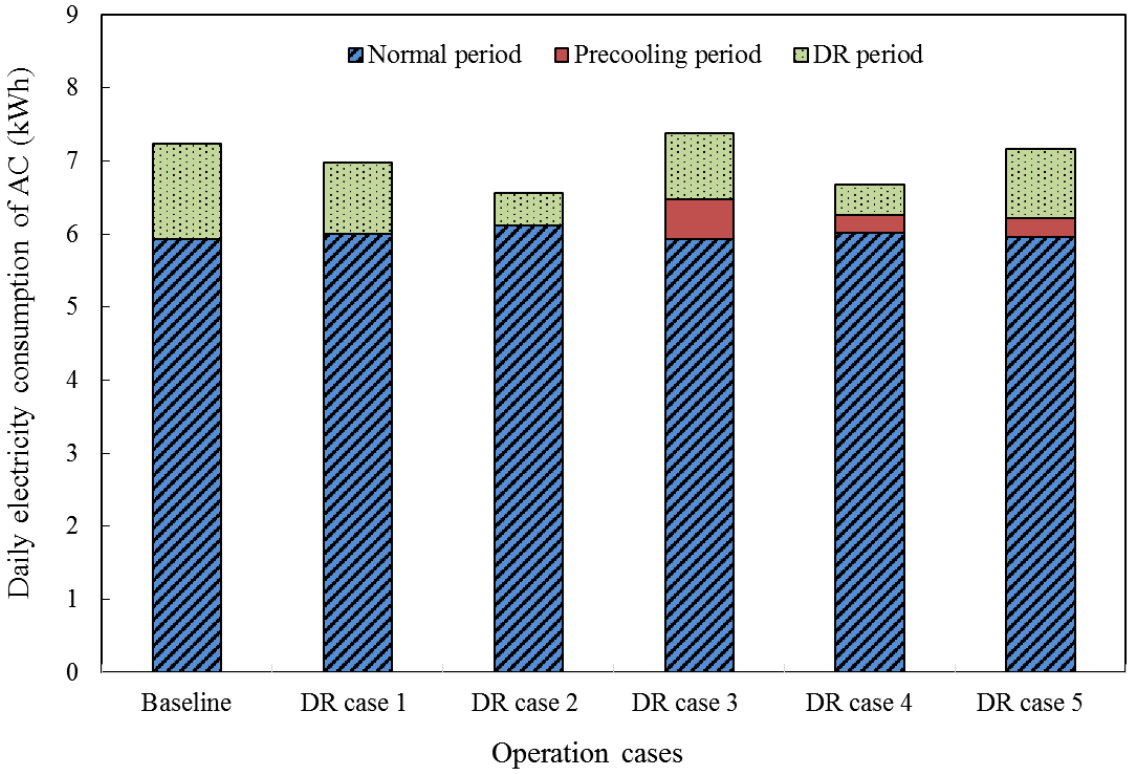

Fig. 10. AC electricity consumption in the baseline and DR cases.

5. Conclusions

This paper presents a self-learning grey-box room thermal model which can accurately predict the indoor air temperature. Three popular optimization techniques are adopted to optimize the R and C values and their performances are compared. Pre-process of model parameters is introduced to improve the accuracy and computational efficiency. The potential benefits of two types of DR strategies are investigated using the grey-box room thermal model and a simplified AC energy consumption model.

The developed grey-box room thermal model can be trained by making full use of the data available in the home energy management system. It can be embedded in the system for optimal home load scheduling in response to DR signals. A self-learning model is important considering that the model-based optimal load scheduling is the most promising DR strategy for residential DR-enabled ACs in

smart grids. A room thermal model with fixed parameter values is not applicable to a diversity of high-rise residential buildings in different cities because the building materials, architecture design and occupant habits are very different. The model developed in this work is valuable to HEMS manufacturers in developing DR strategies for residential ACs. The electric utilities can also use the model to evaluate the DR programs and make corresponding incentive policies before practical implementations of the DR programs. Simulation results show that temperature set-point reset combined with precooling strategy can result in more than 26% power reduction during the DR hours on a typical summer day in Hong Kong. The two types of DR strategies of ACs can help to reduce the power grid loads during the peak demand periods, especially when large quantities of air conditioners response simultaneously.

The air conditioner in this study uses a single-speed compressor, and its power consumption model is a simplified empirical model. However, residential inverter-driven air conditioners are becoming popular and have been widely installed in residential buildings nowadays. In the future, we will focus on the development of an integrated thermal response model which combines inverter-driven AC and building thermal mass. The model-based optimal load scheduling strategies will be developed to enable residential ACs to participate in the grid operation and contribute to the balance of supply and demand in smart grid.

Acknowledgement

The research presented in this paper is financially supported by a grant (ECS/533212) of the Research Grant Council (RGC) of the Hong Kong SAR.

References

[1] Ipakchi A, Albuyeh F. Grid of the future. Power and Energy Magazine, IEEE. 2009;7:52-62.

[2] Boroojeni KG, Amini MH, Iyengar S. Smart Grids: Security and Privacy Issues. Springer; 2016.

[3] Siano P. Demand response and smart grids—A survey. Renewable and Sustainable Energy Reviews. 2014;30:461-78.

[4] Nolan S, O'Malley M. Challenges and barriers to demand response deployment and evaluation. Applied Energy. 2015;152:1-10.

[5] Tang R, Wang S, Gao D-C, Shan K. A power limiting control strategy based on adaptive utility function for fast demand response of buildings in smart grids. Science and Technology for the Built Environment. 2016;22:810-9.

[6] Broeer T, Fuller J, Tuffner F, Chassin D, Djilali N. Modeling framework and validation of a smart grid and demand response system for wind power integration. Applied Energy. 2014;113:199-207.

[7] Rajeev T, Ashok S. Dynamic load-shifting program based on a cloud computing framework to support the integration of renewable energy sources. Applied Energy. 2015;146:141-9.

[8] U.S. Energy Information Administration. Electric Power Annual 2015. Washington, DC: U.S. Department of Energy; 2016.

[9] Federal Energy Regulatory Commission. A national assessment of demand response potential. 2009.

[10] Haider HT, See OH, Elmenreich W. A review of residential demand response of smart grid. Renewable and Sustainable Energy Reviews. 2016;59:166-78.

[11] Siano P, Sarno D. Assessing the benefits of residential demand response in a real time distribution energy market. Applied Energy. 2016;161:533-51.

[12] Amini M, Frye J, Ilić MD, Karabasoglu O. Smart residential energy scheduling utilizing two stage mixed integer linear programming. North American Power Symposium (NAPS), 2015: IEEE; 2015. p. 1-6.

[13] Swan LG, Ugursal VI. Modeling of end-use energy consumption in the residential sector: A review of modeling techniques. Renewable and Sustainable Energy Reviews. 2009;13:1819-35.

[14] Kamyab F, Amini M, Sheykhha S, Hasanpour M, Jalali MM. Demand response program in smart grid using supply function bidding mechanism. IEEE Transactions on Smart Grid. 2016;7:1277-84.

[15] Amini MH, Nabi B, Haghifam M-R. Load management using multi-agent systems in smart distribution network. Power and Energy Society General Meeting (PES), 2013 IEEE: IEEE; 2013. p. 1-5.

[16] Taniguchi A, Inoue T, Otsuki M, Yamaguchi Y, Shimoda Y, Takami A, et al. Estimation of the contribution of the residential sector to summer peak demand reduction in Japan using an energy end-use simulation model. Energy and Buildings. 2016;112:80-92.

[17] Widergren S, Subbarao K, Chassin D, Fuller J, Pratt R. Residential real-time price response simulation. Power and Energy Society General Meeting, 2011 IEEE: IEEE; 2011. p. 1-5.

[18] Lujano-Rojas JM, Monteiro C, Dufo-López R, Bernal-Agustín JL. Optimum residential load management strategy for real time pricing (RTP) demand response programs. Energy Policy. 2012;45:671-9.

[19] Molina D, Lu C, Sherman V, Harley RG. Model predictive and genetic algorithm-based optimization of residential temperature control in the presence of time-varying electricity prices. Industry Applications, IEEE Transactions on. 2013;49:1137-45.

[20] Yoon JH, Bladick R, Novoselac A. Demand response for residential buildings based on dynamic price of electricity. Energy and Buildings. 2014;80:531-41.

[21] Li S, Zhang D, Roget AB, O'Neill Z. Integrating home energy simulation and dynamic electricity price for demand response study. Smart Grid, IEEE Transactions on. 2014;5:779-88.

[22] Katipamula S, Lu N. Evaluation of residential HVAC control strategies for demand response programs. ASHRAE Transctions. 2006;112:535.

[23] Lu N. An evaluation of the HVAC load potential for providing load balancing service. Smart Grid, IEEE Transactions on. 2012;3:1263-70.

[24] Thomas AG, Jahangiri P, Wu D, Cai C, Zhao H, Aliprantis DC, et al. Intelligent residential air-conditioning system with smart-grid functionality. Smart Grid, IEEE Transactions on. 2012;3:2240-51.

[25] Zhang W, Lian J, Chang C-Y, Kalsi K. Aggregated modeling and control of air conditioning loads for demand response. Power Systems, IEEE Transactions on. 2013;28:4655-64.

[26] Pacific Northwest National Laboratory. GridLAB-D software. Available from: http://gridlab-d.sourceforge.net/wiki/index.php/Main_Page.

[27] Pratt RG, Conner CC, Drost MK, Miller NE, Cooke BA, Halverson MA, et al. Significant ELCAP analysis results: Summary report. [End-use Load and Consumer Assessment Program]. 1991. p. Medium: ED.

[28] Seem JE. Modeling of heat transfer in buildings: Wisconsin Univ., Madison (USA); 1987.

[29] ASHRAE. ASHRAE Handbook: Fundamentals (SI Edition). Atlanta, GA: American Society of Heating, Refrigerating and Air-conditioning Engineers; 2009.

[30] Lam JC, Tsang CL, Li DHW, Cheung SO. Residential building envelope heat gain and cooling energy requirements. Energy. 2005;30:933-51.

[31] Lam JC, Lun IY, Li DH. Long-term wind speed statistics and implications for outside surface thermal resistance. Architectural Science Review. 2000;43:95-100.

[32] Domínguez-Muñoz F, Cejudo-López JM, Carrillo-Andrés A. Uncertainty in peak cooling load calculations. Energy and Buildings. 2010;42:1010-8.

[33] BRE. The Governments Standard Assessment Procedure for Energy Rating of Dwellings. Watford, DEFRA; 2012.

[34] Nocedal J, Wright S. Numerical optimization: Springer Science & Business Media; 2006.

[35] Wang S, Xu X. Parameter estimation of internal thermal mass of building dynamic models using genetic algorithm. Energy Conversion and Management. 2006;47:1927-41.

[36] Tuhus-Dubrow D, Krarti M. Genetic-algorithm based approach to optimize building envelope design for residential buildings. Building and Environment. 2010;45:1574-81.

[37] Xuemei L, Lixing D, Yan L, Gang X, Jibin L. Hybrid genetic algorithm and support vector regression in cooling load prediction. Knowledge Discovery and Data Mining, 2010 WKDD'10 Third International Conference on: IEEE; 2010. p. 527-31.

[38] Kusiak A, Xu G, Tang F. Optimization of an HVAC system with a strength multi-objective particle-swarm algorithm. Energy. 2011;36:5935-43.

[39] Chassin DP, Stoustrup J, Agathoklis P, Djilali N. A new thermostat for real-time price demand response: Cost, comfort and energy impacts of discrete-time control without deadband. Applied Energy. 2015;155:816-25.

[40] Yoon JH, Baldick R, Novoselac A. Demand response control of residential HVAC loads based on dynamic electricity prices and economic analysis. Science and Technology for the Built Environment. 2016;22:705-19.

[41] York DA, Tucker EF. DOE-2 Reference Manual Part 1 Version 2.1. Los Alamos, New Mexico: Los Alamos Scientific Laboratory; 1980.

[42] ANSI/AHRI. Standard for Performance Rating of Unitary Air-Conditioning and Air-Source Heat Pump Equipment. Arlington, VA: Air-Conditioning, Heating, and Refrigeration Institute; 2008.